

Wind Loads on a Bottom-mounted Offshore Wind Turbine Tower

Kazumasa OKUBO⁺¹, Manabu YAMAMOTO⁺², Yukinari FUKUMOTO⁺³ and Takeshi ISHIHARA⁺⁴
⁺¹⁺²Kajima Technical Research Institute, Tokyo, Japan
⁺³Tokyo Electric Power Company Research & Development Center, Yokohama, Japan
⁺⁴The University of Tokyo, Tokyo, Japan

Having a long coastline, offshore wind energy is one of the most important solutions for the increase of renewable energy in Japan. However, due to the differences in wind, marine and earthquake conditions between Japan and Europe, the safety, the environmental impact and the economic feasibility of offshore wind energy have to be investigated. Since 2009, the authors have started an experimental investigation of NEDO's offshore wind power generation system proving research project on the Pacific Ocean near coast of Japan. This project aims to establish an offshore wind power generation technology which is suitable for Japanese external conditions. This paper describes the characteristics of wind loads on the offshore wind turbine tower. The site is located at 3.1km offshore from Choshi, and the water depth is 11.9m. Proving wind turbine is a propeller-type with three blades (Hub height: 80m, Rated power: 2.4MW, Bottom-mounted). The wind loads were investigated as bending moment at bottom of tower by using strain-gauge data. In this paper, obtained wind loads were compared between operational condition and feathering condition, wind of the landside and of the seaside. As a result, in both condition, the maximum wind loads for the wind of the landside were bigger than those for the wind of the seaside under the influence of the land 3.1 kilometers away from the wind turbine. The gust effect factors in the feathering condition for the wind of the seaside were from 1.8 to 2.0. Furthermore, the gust effect factors for the wind of the landside were more than 2.1 in range of less than 30m/s.

Keyword: offshore wind turbine, field measurement, wind load, gust effect factor

1. Introduction

Most of the wind power generation systems in Japan are sited on land. Offshore wind power generation systems, however, are expected to go into widespread use in the coming years because higher wind speed compared with on-land make it possible to obtain more stable power output and also because large wind turbines and large-scale wind farms can be constructed. In order to establish the technology to build bottom-mounted offshore wind turbine towers capable of withstanding harsh meteorological and oceanographic characteristic of Japan in preparation for the proliferation of offshore wind power generation systems, New Energy and Industrial Technology Development Organization (NEDO) and Tokyo Electric Power Company constructed the first bottom-mounted offshore wind turbine tower¹⁾ in Japan off the coast of Chiba Prefecture under their joint demonstration project. In this paper, the study conducted to estimate bending moments (wind loads) acting on the base of the bottom-mounted wind turbine tower from strain measurement data, and investigate wind load characteristics peculiar to wind turbines and the influence of turbulence on wind loads.

2. Observation System

The structure is a bottom-mounted offshore wind turbine tower constructed 3.1 km to the south of Choshi City, Chiba Prefecture¹⁾ as shown in Figure 1. A wind observation tower has also been built 285m to the east of the wind turbine^{1),2)}. Figure 2 illustrates the offshore wind turbine. Strain gauges were installed to

⁺¹okubokaz@kajima.com, ⁺²yamamoto-ma@kajima.com, ⁺³fukumoto.yukinari@tepco.co.jp, ⁺⁴ishihara@bridge.t.u-tokyo.ac.jp

the internal wall surface of the tower at the three different levels shown in Figure 2. Strain (in the vertical direction) was measured at a sampling frequency of 50Hz. After subtracting the strain under windless conditions (zero-strain point) from the strain under wind loading, the measured strain thus obtained was converted to a combination of an along-wind strain and an across-wind strain by using trigonometric functions based on the 10-minute mean wind direction obtained from the wind vane anemometer installed on top of the nacelle (M.S.L. + approx. 84m). This study turns attention to the along-wind bending moment $M_D(t)$ and the across-wind bending moment $M_L(t)$ at the base of the tower [the top of the foundation + 0.77m (M.S.L. + 10.9m)]. $M_D(t)$ and $M_L(t)$ were calculated by using the following equation:

$$M_D(t) = \frac{EI\{\varepsilon_W(t) - \varepsilon_L(t)\}}{D'}, \quad M_L(t) = \frac{EI\{\varepsilon_{Lr}(t) - \varepsilon_{Ll}(t)\}}{D'} \tag{1}$$

$$I = \frac{(D^4 - D'^4)\pi}{64} \tag{2}$$

where E : Young's modulus for the tower, I : moment of inertia of area of the tower, $\varepsilon_W(t)$ / $\varepsilon_L(t)$: along-wind strain on the windward / leeward side at time t , $\varepsilon_{Lr}(t)$ / $\varepsilon_{Ll}(t)$: across-wind strain on the right / left side at time t , D' : inside diameter of the tower, D : outside diameter of the tower

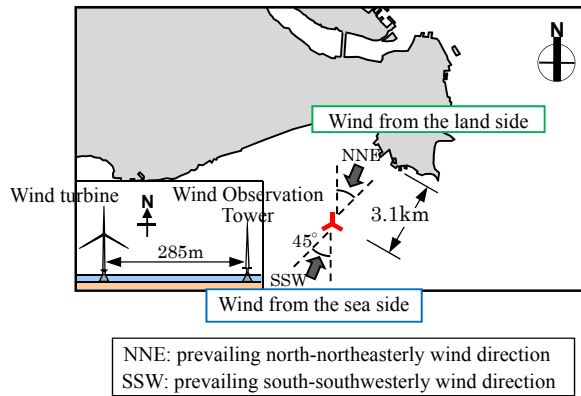


Figure 1: Offshore wind power generation system site

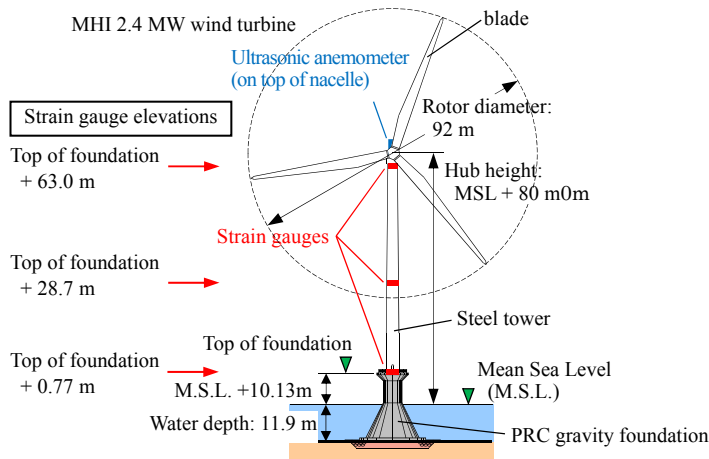


Figure 2: Offshore wind power generation system and strain gauges installed to the wind turbine tower

10-minute mean wind speed was calculated from wind speed obtained on the top of the nacelle. The observed wind speed was corrected to hub-height wind speed (hereinafter referred to simply as "wind speed")

by using the wind speed measurement data obtained from the wind observation tower (M.S.L. + 80m). Figure 3 shows the relationship between the mean wind speeds at the nacelle and the wind observation tower and the wind speed conversion formulas used. Turbulence intensities of wind from the land side and wind from the sea side were about 9% and 5%, respectively²⁾. In the vibration tests conducted by using the excitation system installed in the tower, the first-mode natural frequency and the first-mode damping ratio in the tower main shaft direction (along-wind direction) were 0.35Hz and 0.2%, respectively³⁾.

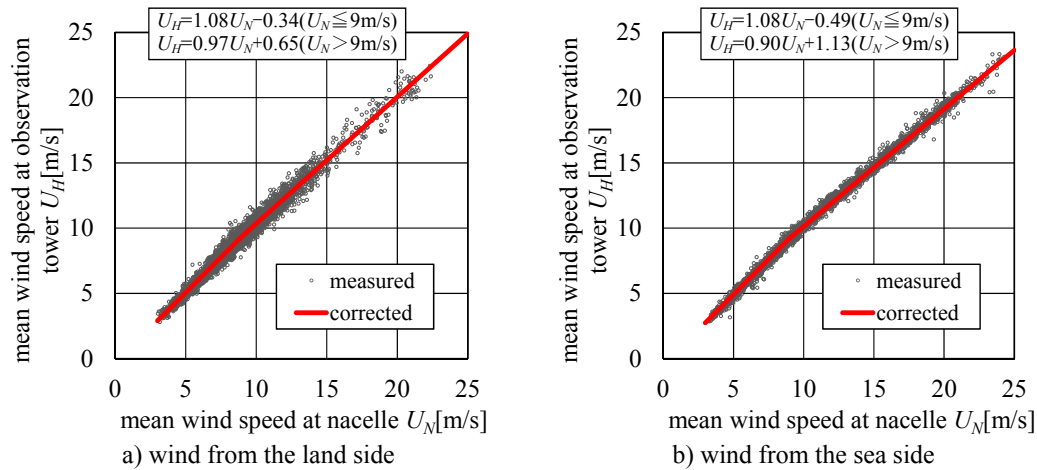


Figure 3: Mean wind speeds at Nacelle and at Wind Observation Tower

3. Observation Results

(1) Test to identify zero-strain point under windless conditions

Since wind turbine yaw control adjusts the turbine blade rotation plane so that it squarely faces the wind, vertical strain changes depending on the direction of the nacelle, which is a heavy component. A test, therefore, was conducted under arbitrarily varied nacelle direction conditions to identify the zero-strain point under windless conditions. The test was conducted under low wind conditions (3 to 5m/s) and the turbine blades were feathered (so that they did not rotate) during the test so as to minimize the wind force acting on the tower. In order to eliminate the influence of thermally induced elongation due to sunlight on strain, the test was carried out at night. Figure 4 shows an example of the relationship between nacelle direction and the zero-strain point based on the data obtained from the strain gauges on the north side. As shown, the zero-strain point changes depending on nacelle direction: in the case where the nacelle is directed to the north, in which the strain gauge position coincides with the rotor direction, the zero point shifts toward the compression side, and in the case where the nacelle is directed to the south (in the opposite direction), the zero point shifts toward the tension side. Figure 4 also shows nighttime observation data obtained when the wind speed was lower than 1m/s. As shown, the nighttime observation data show close agreement with the test results. It was decided, therefore, to use those test results to define the zero-strain point under windless conditions.

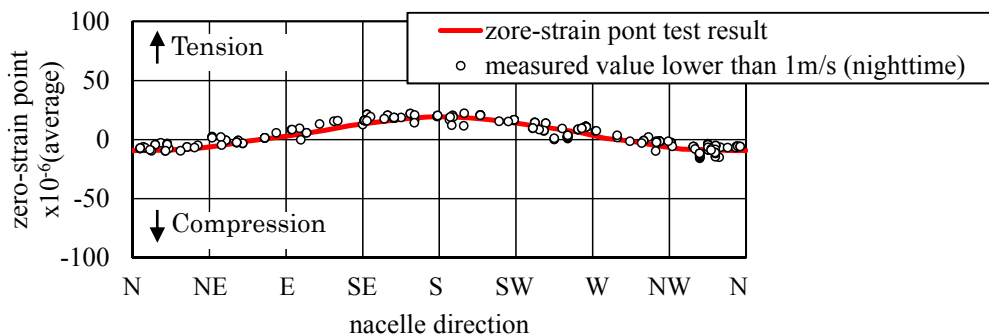


Figure 4: nacelle direction and zero-strain point (example of strain gauge on the north side)

(2) Wind load in operational condition

Figure 5 shows the relationship between wind speed and the along-wind static bending moment (10-minute average) M_D in operational condition. Figure 6 shows the relationship between wind speed and the maximum bending moment (10-minute maximum instantaneous value) M_{Dmax} . To show the differences in the turbulence intensity of approaching flows, Figures 5 to 7 show the values for the wind from the sea side and the wind from the land side defined in Figures 1. The shown values are nighttime observation data that are relatively unaffected by thermally induced elongation due to sunlight. As shown, M_D increases with wind speed when wind speed is not higher than 10m/s. When wind speed exceeds 11m/s, however, M_D begins to decrease. This is a wind load characteristic peculiar to wind turbines. The reason for this is as follows. When wind speed is 10m/s or lower, the blade pitch angle (the angle between the chord line and the rotor plane) is kept small and constant, and at wind speeds of 5 to 8m/s, the rotor speed is increased as wind speed increases. When wind speed is higher than 11m/s, the rotor speed is kept constant and the pitch angle is increased as wind speed increases (pitch control)⁴⁾. Although M_D values show fair agreement between wind from the land side and wind from the sea side, M_{Dmax} values for wind from the land side are greater than those for wind from the sea side, indicating the influence of turbulence intensity. The influence of turbulence intensity was evaluated quantitatively by determining the gust effect factor $G_D (= M_{Dmax}/M_D)$ for along-wind loads. The G_D values shown in Figure 7 are smallest at a wind speed of about 10m/s at which M_D is maximized. At wind

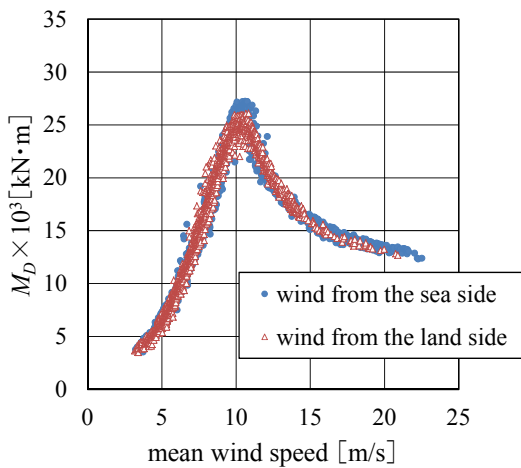


Figure 5: Along-wind static bending moment M_D (operational condition)

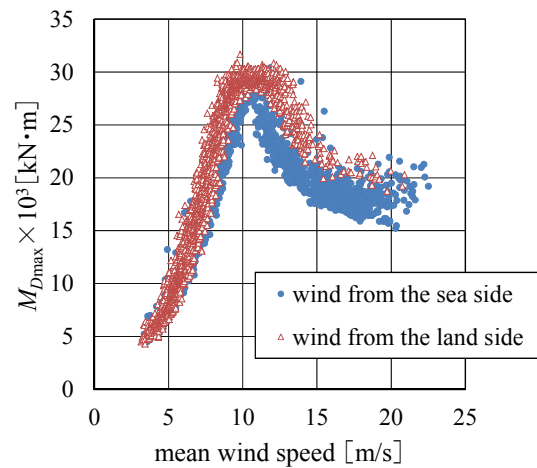
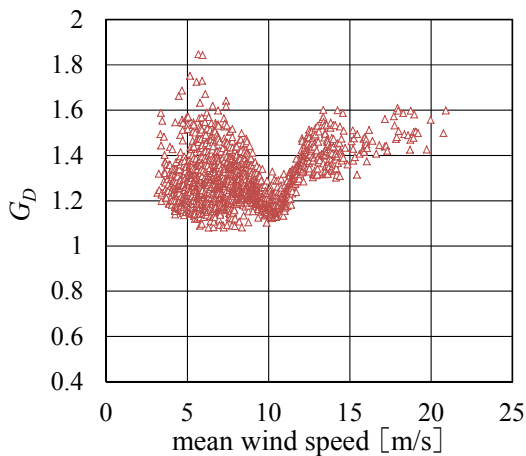
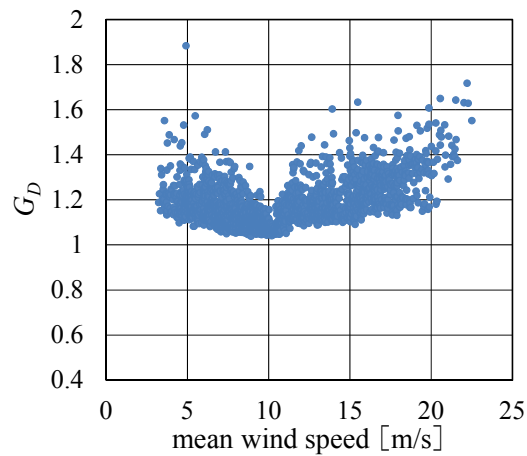


Figure 6: Along-wind maximum bending moment M_{Dmax} (operational condition)



a) wind from the land side



b) wind from the sea side

Figure 7: Along-wind gust effect factor G_D (operational condition)

speeds of 11m/s or higher, G_D tends to increase with wind speed. The values of G_D for wind from the land side tends to be greater than the values for wind from the sea side: G_D values for wind from the land side at a wind speed of 10m/s range from 1.1 to 1.3, and values for wind from the sea side range from 1.05 to 1.1.

(3) Wind load in feathering condition

Figure 8 shows the relationship between wind speed and the along-wind static bending moment M_D in feathering condition. Figure 9 shows the relationship between wind speed and the maximum bending moment M_{Dmax} . Figure 10 shows the relationship between wind speed and the maximum across-wind bending moment M_{Lmax} . To show the differences in the turbulence intensity of approaching flows, Figures 8 to 10 show the values for the wind from the sea side and the wind from the land side defined in Figures 1. The shown values are nighttime observation data that are relatively unaffected by thermally induced elongation due to sunlight. The wind speed range considered in this study is 1 to 29m/s, and the Reynolds numbers range from 3×10^5 to 7×10^6 (the reference length is 3.5m, which is the average width of the tower).

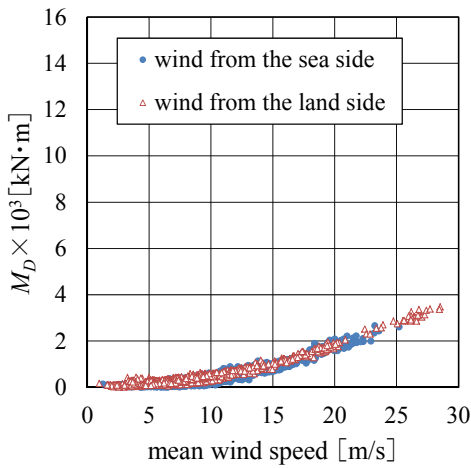


Figure 8: Along-wind static bending moment M_D (feathering condition)

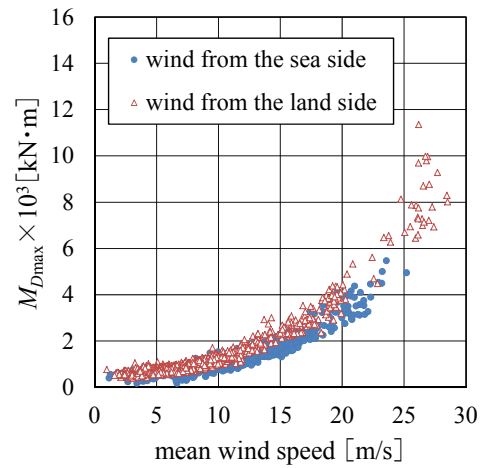


Figure 9: Along-wind maximum bending moment M_{Dmax} (feathering condition)

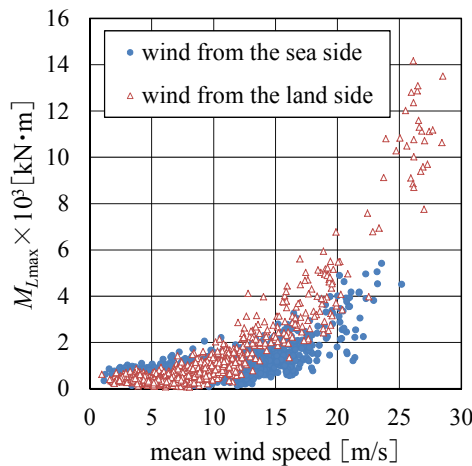


Figure 10: Across-wind maximum bending moment M_{Lmax} (feathering condition)

As shown, M_D increases with wind speed, and the values for wind from the sea side and the values for wind from the land side are similar. The M_{Dmax} and M_{Lmax} values for wind from the land side are greater than those for wind from the sea side, showing the influence of the turbulence intensity of approaching flows. The clear peak of M_{Lmax} which seems vortex induced vibration wasn't seen. Comparison of the values in the

along-wind direction (M_{Dmax}) and the values in the across-wind direction (M_{Lmax}) reveals that M_{Lmax} tends to be greater than M_{Dmax} in the wind speed range higher than 15m/s.

The along-wind static bending moment coefficient C_{MD} was calculated by using the formula shown below. Figure 11 shows the relationship between wind speed and C_{MD} . As shown, C_{MD} gradually approaches approximately 0.42 as wind speed increases.

$$C_{MD} = \frac{M_D}{0.5\rho U_H D H'^2} \tag{3}$$

where ρ : air density, D : average width of the tower, H' : distance between strain measurement height and hub height

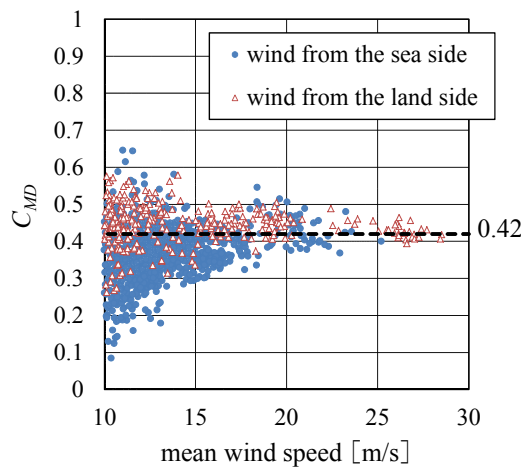


Figure 11: Along-wind static bending moment coefficient C_{MD} (feathering condition)

Figure 12 shows the relationship between wind speed and the gust effect factor G_D . Figure 12 also shows the G_D values specified in the Guidelines for Design of Wind Turbine Support Structures and Foundations⁵⁾. As shown, as wind speed increased, the G_D of wind from the sea side showed values of about 1.8 to 2.0, which correspond to category of surface roughness I or II defined in the Guideline. The G_D of wind from the land side ranged from 2.0 to 3.5 at wind speeds higher than 20m/s, showing values falling into category of surface roughness III or higher. Since the maximum wind speed observed was about 1/2 of the design wind speed, it is necessary to accumulate higher-wind-speed data.

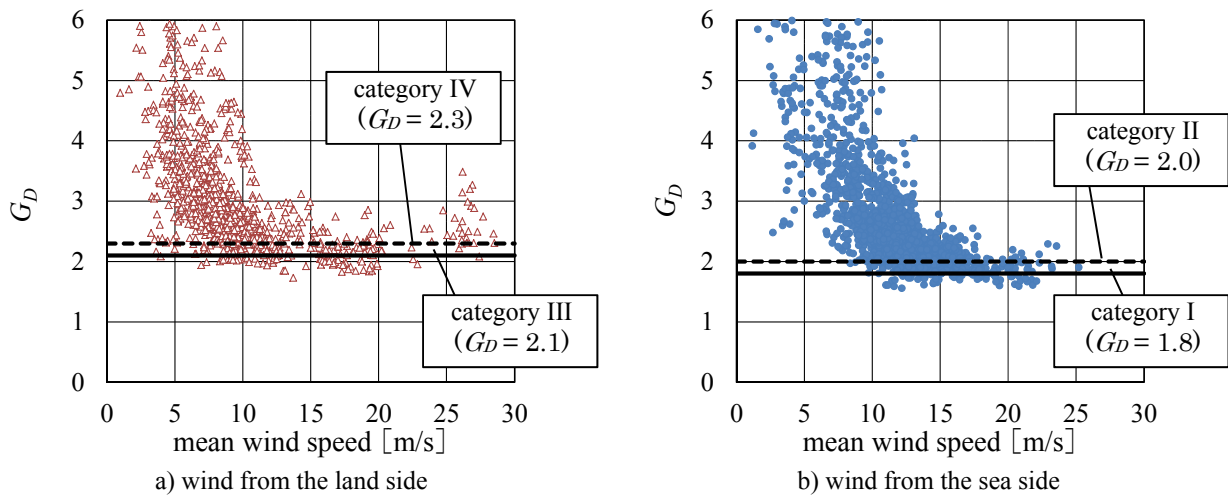


Figure 12: Along-wind gust effect factor G_D (feathering condition)

(4) Comparison between operational condition and feathering condition

M_{Dmax} in operational condition and M_{Dmax} in feathering condition are compared. Figure 13 shows the relationship between wind speed and M_{Dmax} . Figure 13 also shows predicted values in feathering condition calculated by using the C_{MD} values shown in Figure 11 and the G_D values shown in Figure 12. As shown, at wind speeds below the cut-out wind speed, the M_{Dmax} values in feathering condition are substantially smaller than the values in operational condition, but M_{Dmax} is expected to increase as wind speed increases. It is thought likely that at the design wind speed (with a return period of 50 years) shown in Figure 13, M_{Dmax} values in feathering condition will be similar to the values in operational condition.

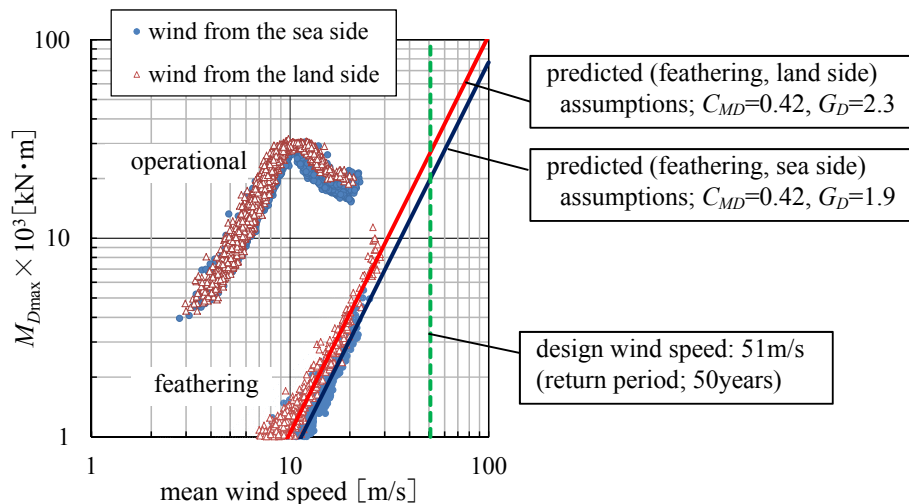


Figure 13: Comparison between operational and feathering condition about M_{Dmax}

4. Conclusion

Focusing on the first bottom-mounted offshore wind turbine tower in Japan, this study investigated wind load characteristics and the influence of turbulence intensity on wind loads. As a result, it has been clarified that the zero-strain point of the tower changes depending on nacelle direction, and that since wind loads are affected by land-induced turbulence even though the tower is located at a distance of 3.1 km from the nearest land, loads induced by wind from the land side are greater than by wind from the sea side. It has also been clarified that the gust effect factor of wind from the sea side in feathering condition ranges from 1.8 to 2.0 (category of surface roughness I or II defined in the JSCE Guideline), and the gust effect factor of wind from the land side shows 2.1 or larger values (category of surface roughness III or higher) at wind speeds lower than 30m/s.

ACKNOWLEDGMENT

The authors would like to gratefully acknowledge that this study was conducted as part of a study commissioned by New Energy and Industrial Technology Development Organization (NEDO).

REFERENCES

- 1) Yukinari Fukumoto, Takeshi Ishihara, Kazumasa Okubo, Koji Hayashida : Empirical Research of Bottom Mounted Offshore Wind Turbine, *Wind Engineers, JAWE*, Vol.36, No.1(No.126), pp.4-8, 2011
- 2) Hiroyuki Sukegawa, Yukinari Fukumoto, Toru Yamanaka, Kazumasa Okubo, Takeshi Ishihara : An Offshore Wind Observation at a Point of 3.1km off Choshi, *Japan Wind Energy Symposium*, Vol. 35, pp.260-263, 2013
- 3) Atsushi Yamaguchi, Sho Oh, Takeshi Ishihara : System identification of an offshore wind turbine based on ambient and forced vibration, *Japan Wind Energy Symposium*, Vol. 35, pp.264-267, 2013
- 4) Manabu Yamamoto, Yukio Naito, Koji Kondo, Takeshi Ohkuma : Wind Loads and External Forces on a

Wind Turbine Tower Based on Field Measurements, *Journal of Structural and Construction Engineering*, No.617, pp.39-46, 2007

- 5) Japan Society of Civil Engineers : Guidelines for Design of Wind Turbine Support Structures and Foundations, 2010